



# MECHANICAL PROPERTIES OF GEO-MATERIALS USED FOR CONSTRUCTING EARTHEN WALLS IN JAPAN

Hiroyuki ARAKI<sup>1</sup>, Junichi KOSEKI<sup>2</sup> and Takeshi SATO<sup>3</sup>

**ABSTRACT:** A rammed earth technique is a traditional architectural technique to build soil structures by compressing geo-materials in a form. In this study, the mechanical properties of traditional rammed earth material are evaluated by conducting some laboratory tests. Their unconfined compression strength increases with decrease of the water content; their unconfined tension strength is approximately 10 % of the unconfined compression strength; no significant reduction in the peak strengths of specimens subjected to large amplitude cyclic loading is observed.

**Key Words:** rammed earth, compression strength, tensile strength, cyclic loading

## INTRODUCTION

Rammed earth technique is a traditional construction technique to build soil structures by compressing clay, sand and gravel in a form. This technique, which had already been used in Yellow River Valley, China around B.C. 2000 in Asia region (Onizuka et al. 2007), is used for walls of a house all over the world still now. In recent years, rammed earth construction is attracting an interest in construction projects of modern housing due to some advantages, e.g. its high capability for humidity control, potential for recycling, a reduction in construction energy, among others (Minke 2006). The compression strength of various rammed earth materials (e.g. Hall and Djerbib 2004, Jayasinghe and Kamaladasa 2007, Rendell and Jauberthie 2009) and thermal conductivity of rammed earth walls (e.g. Hall and Allinson 2009, Lee et al. 2010) are studied in order to apply a rammed earth wall to a modern housing. However, seismic behavior of a rammed earth wall has not been investigated sufficiently. Evaluation of seismic safety of a rammed earth wall is required in conducting an appropriate design of a newly built wall in earthquake-prone countries like Japan.

On the other hand, old rammed earth structures exist all over the world. For example, Rendell and Jauberthie (2009) reported that some housings and agricultural housings, which were in excess of 100 years old in east Brittany, France, were generally in a good state of repair. In Japan, rammed earth technique was used for a wall surrounding a temple and a shrine, such as “Abura-dobei” wall in Ryoan-ji temple in Kyoto, “Taikou-bei” wall in Sanju-sangen-do temple in Kyoto, “Ooneri-bei” wall in Nishinomiya shrine in Kobe and “Oo-gaki” wall in Horyu-ji in Nara (**Photo 1**); these walls have been registered as the important cultural properties by Japanese government.

Japanese government's Central Disaster Management Council (2009) released that many important cultural properties in the Kansai region in Japan had a possibility of suffering earthquake with a Japanese seismic intensity of 6 in some scenario. In fact, a part of “Ooneri-bei” wall in Nishinomiya

<sup>1</sup> Ph.D. student, Department of Civil Engineering, University of Tokyo

<sup>2</sup> Professor, Institute of Industrial Science, University of Tokyo

<sup>3</sup> Technical Director, Integrated Geotechnology Institute Ltd.



**Photo 1.** The rammed earth wall (“Oo-gaki”) surrounding Horyu-ji temple in Nara.



**Photo 2.** The rammed earth wall (“Oo-neri bei” in Nishinomiya shrine) collapsed by the Great Hanshin Earthquake Disaster. This photo was taken on January 17 1995 (by courtesy of Nishinomiya City)

shrine collapsed in the Great Hanshin Earthquake Disaster in 1995 (**Photo 2**). Therefore effective construction and seismic measures need to be established in order to pass on these important cultural properties to next generations.

In a relevant previous study, it was estimated that tensile failure at a bottom part of a rammed earth wall causes over-turning of the wall in earthquakes (Takadachi and Koshihara 2010). Hence tensile strength is an important factor for evaluation of seismic behavior. Furthermore, shear properties of a rammed earth material are required in order to analyze numerically the seismic behavior of cultural properties where nondestructive evaluation shall be also carried out.

In this study, the mechanical properties of rammed earth materials are evaluated by unconfined compression tests, tri-axial compression test and unconfined tension tests. For the unconfined compression tests and unconfined tension tests, not only monotonic loading but also cyclic loading are applied. The rammed earth material employed in this study is traditional material used for very old wall in a certain temple in Japan.

## TEST CONDITION AND PROCEDURE

### *Rammed earth material*

A geo-material that was composed of clayey sand and silty sand was used for a reconstruction project of rammed earth walls surrounding a traditional Japanese temple. In this study, this rammed earth material was employed for a series of a series of laboratory tests.

The clayey sand was made from the old rammed walls by crushing and sieving. The silty sand was a commercial soil that had been frequently used for earthen walls in Japan. Their particle size distributions are shown in **Fig. 1**. The grain size distribution of the clayey sand was wide. The clayey soil and the silty sand contained fines content of 48.4 % and 19.2 %, respectively.

The mixing proportion of the material is shown in **Table 1**. The mixing ratio of the dry weight of the clayey sand to the silty sand of the material was determined by referring to the mixing ratio used in the aforesaid reconstruction project. The ratio of the amount of water to the dry weight of the solid enabled to achieve its optimum water content (10.1 %), which was evaluated by modified Proctor compaction tests ( $E = 2700 \text{ kJ/m}^3$ ) (**Fig. 2**).

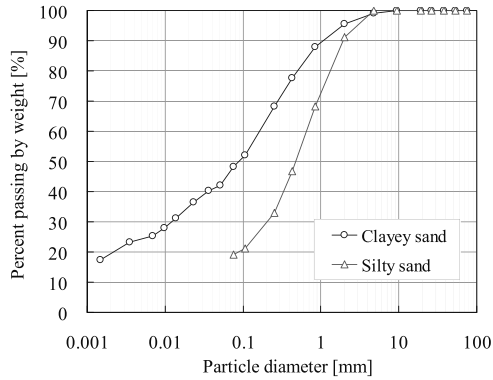


**Figure 1.** Particle size distributions of the material

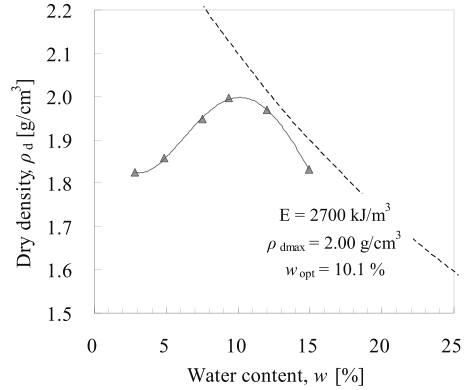


**Figure 2.** Compaction curves of the mixture by modified Proctor tests.

**Table 1.** Mixing proportion of the material by weight

Clayey sand (%)	Silty sand (%)	Water (%)
59.04	31.79	9.17

**Table 2.** Specimens for unconfined compression tests

Series	Curing condition	Curing days
UC1	inside mould without sealing	7, 14, 28, 56, 84, 112, 168
UC2	demoulded without sealing	7, 14, 28, 56
UC3	inside mould with sealing	7, 14, 28, 56

### Unconfined compression tests

In order to conduct unconfined compression tests on the rammed earth material, three series of specimens were prepared by using the mixture shown in **Table 1**. The details of each series are shown in **Table 2**. Each specimen was compacted in a plastic mould with a dimension of 50 mm in inner diameter and 100 mm in height, into ten layers. Based on a weight and a dropping height of a rammer, the required number of blows was assigned in order to apply the same energy of compaction as in the modified Proctor test ( $E = 2700 \text{ kJ/m}^3$ ).

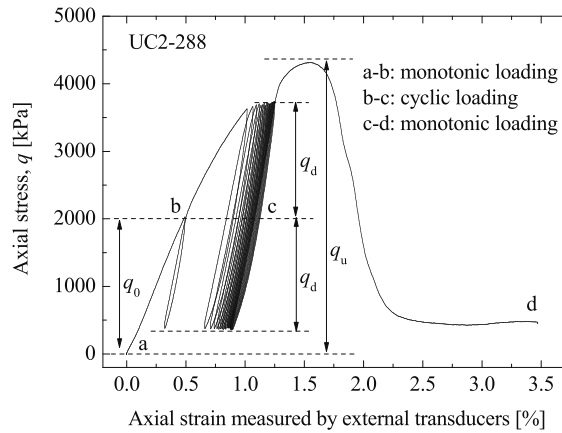
All specimens were cured under atmospheric pressure and room temperature, though some curing conditions were different in each series as follows. The specimens of the series UC1 were cured in the air inside their moulds without sealing. The specimens of the series UC2 were demoulded immediately after compaction, then were cured in the air without sealing. The specimens of the series UC3 were cured inside their mould with sealing with a plastic bag.

On some specimens of the series UC2, cyclic loading tests were conducted. The details of the specimens for cyclic loading tests are shown in **Table 3**, and a typical stress-strain behavior in the cyclic loading test is shown in **Fig. 3**. The water content,  $w$  shown in **Table 3** was measured after tests. In **Fig. 3**, initial and final portions (a-b and c-d) are monotonic loading part and middle portion (b-c) is cyclic loading part. The value of the initial stress,  $q_0$  was set at about 40 to 50 % of the peak stress,  $q_u$ , which was estimated based on the results of monotonic compression test (**Table 3**, UC-2-283, 284, 285). The single-amplitude value of the cyclic stress,  $q_d$  was set at 80 % of  $q_0$ .

In all the unconfined compression tests, which include monotonic and cyclic tests, the axial strain rate was set to 1 %/min. The axial displacement was measured by two external displacement transducers (EDTs) set at diametrically opposed positions and a pair of local deformation transducers (LDTs, Goto et al. 1991) attached on the specimen. In order to reduce the effects of bedding error at the interfaces between the specimen and a top cap and a pedestal, capping was made by using gypsum.

**Table 3.** Details of specimens for unconfined cyclic compression tests

No.	Loading type	Curing time (days)	$w$ (%)	Dry density ( $\text{g}/\text{cm}^3$ )	$q_0$ (kPa)	$q_d$ (kPa)	Number of cycles
UC2-283	Monotonic	28	1.13	1.971	-	-	-
UC2-284	Monotonic	28	1.11	1.950	-	-	-
UC2-285	Monotonic	28	1.24	1.958	-	-	-
UC2-286	Cyclic	28	1.14	1.964	1500	1200	20
UC2-287	Cyclic	28	1.18	1.958	2000	1600	20
UC2-288	Cyclic	28	1.15	1.958	2000	1600	20

**Figure 3** Typical stress-strain relationship in unconfined cyclic compression test (UC2-288)**Table 4.** Details of specimens for tri-axial compression tests

No.	Curing time (days)	$w$ (%)	Dry density ( $\text{g}/\text{cm}^3$ )	Confining stress (kPa)
TC-11	28	1.64	1.989	20
TC-12	62	1.46	1.988	50
TC-13	28	1.65	1.993	100
TC-14	55	1.57	1.991	200
TC-15	56	1.49	1.993	400

### Tri-axial compression tests

In order to conduct tri-axial compression tests, five specimens were prepared by using the mixture shown in **Table 1**. The method of making and curing a specimen is identical to that of the series UC2 of the unconfined compression tests. The specimen details are shown in **Table 4**. The results of unconfined compression tests showed that the strength did not depend on the curing time but on the water content,  $w$  the strength depended predominantly on not the curing days but its  $w$  as would be described later, thus the curing time was not necessarily the same.

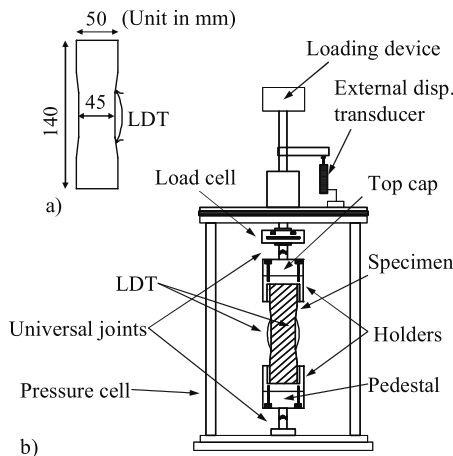
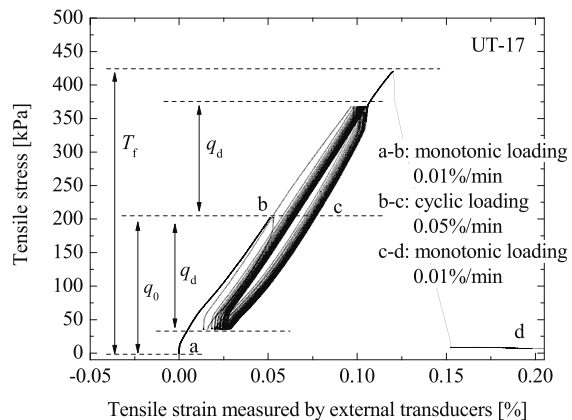
The tests were carried out under drained and unsaturated condition. The water content of specimens measured after tests is shown in **Table 4**. A constant axial strain rate of 1 %/min was employed as in the unconfined compression tests. The axial displacement was measured by two EDTs set at diametrically opposed positions and a pair of LDTs attached on the specimens.

### Unconfined tension tests

In order to conduct unconfined tension tests, eight specimens were prepared by using the mixture shown in **Table 1**. The compacting method for making specimens was identical to that of the unconfined compression tests, except for the specimen shape and dimensions that were cylindrical with a diameter of 50 mm and a height of 140 mm, while the diameter at the middle height was trimmed down to 45 mm (**Fig. 4 a**); this shape was adopted based on the results from finite element

**Table 5.** Details of specimens for unconfined tension tests

No.	Loading type	Curing time (days)	w (%)	Dry density (g/cm <sup>3</sup> )	$q_0$ (kPa)	$q_d$ (kPa)	Number of cycles
UT-11	Monotonic	28	1.58	1.960	-	-	-
UT-12	Monotonic	28	1.55	1.944	-	-	-
UT-13	Monotonic	27	1.46	1.985	-	-	-
UT-14	Monotonic	27	1.54	1.974	-	-	-
UT-15	Monotonic	21	1.11	1.982	-	-	-
UT-16	Monotonic	23	1.23	1.995	-	-	-
UT-17	Cyclic	21	1.22	1.974	200	170	20
UT-18	Cyclic	23	1.36	1.978	200	170	20

**Figure 4.** a) Shape of a specimen for tension test and b) apparatus for unconfined tension test**Figure 5.** Typical stress-strain relationship in unconfined cyclic tension test (UT-17)

analyses in order to avoid failure at the fixed portions in which the tensile stress may be concentrated (Namikawa and Koseki, 2007). The specimens were demoulded and were trimmed down its middle part by a knife immediately after compaction, then were cured in the air without sealing under atmospheric pressure and room temperature for 21 to 28 days. The details of the specimens are shown in **Table 5**.

The apparatus shown in **Fig. 4 b)** was used, without using the pressure cell. The specimens were connected to the holders with epoxy resin. The holders were attached to the top cap and the pedestal, while universal joints were inserted on both ends to reduce the bending moment applied unnecessarily to the specimen.

On two specimens, UT-17 and UT-18, cyclic loading was applied. A typical stress-strain behavior of a cyclic loading test is shown in **Fig. 5**. In **Fig. 5**, initial and final portions (a-b and c-d) are monotonic tensile loading, and middle portion (b-c) is cyclic loading as in unconfined compression tests. The value of the initial tensile stress,  $q_0$  was set at about 50 % of the peak tensile stress,  $T_f$ , which was estimated based on the results of monotonic tension tests (UT-11 to 16). The single-amplitude value of the cyclic stress amplitude,  $q_d$  was set at 85 % of  $q_0$ .

The tensile monotonic strain rate was set to 0.01 %/min at the loading parts of a-b and c-d (**Fig. 5**) and the cyclic strain rate was set to 0.05 %/min at the part of b-c (**Fig. 5**). The axial displacement was measured by two EDTs set at diametrically opposed positions and a pair of LDTs attached on the specimens.

## RESULTS OF UNCONFINED COMPRESSION TESTS

**Figure 6** shows the stress-strain relationships of the series UC1. **Figure 7** shows the stress-strain relationships of the unconfined cyclic compression tests (UC2-286, 287, 288) and the corresponding unconfined monotonic compression tests (UC2-283, 284, 285). The peak strength,  $q_u$ , the water content,  $w$  measured after the test and the stiffness, i.e. the initial tangent modulus,  $E_0$ , and the secant modulus,  $E_{50}$  of series UC1, UC2 and UC3 are shown in **Fig. 8**, **Fig. 9** and **Fig. 10**, respectively.  $E_0$  was evaluated with LDTs at a strain level of about 0.001 % and  $E_{50}$  was evaluated with LDTs also (**Fig. 6**). The results of series UC2 with/without cyclic loading are summarized in **Table 6**.

As for the series UC1, the peak strength gradually increased with the curing time, while the water content decreased (**Figs. 8** and **9**). After 84 days or longer curing time, the peak strength and the water content were stabilized around 2800 kPa and 2.0 %, respectively.

On the other hand, the peak strength and the water content in the series UC2 and UC3 were kept almost constant (**Figs. 8** and **9**). The average values of the peak strength and the water content over all the curing times were around 4200 kPa and 1.24 % in series UC2, respectively and 680 kPa and 9.66 % in series UC3, respectively. Besides, the trends of variations of  $E_0$  and  $E_{50}$  with curing time were similar to those of the peak strength.

In the series UC1 as mentioned above, the peak strength and the stiffness increased with time, while the water content decreased. The properties of peak strength, stiffness and water content of

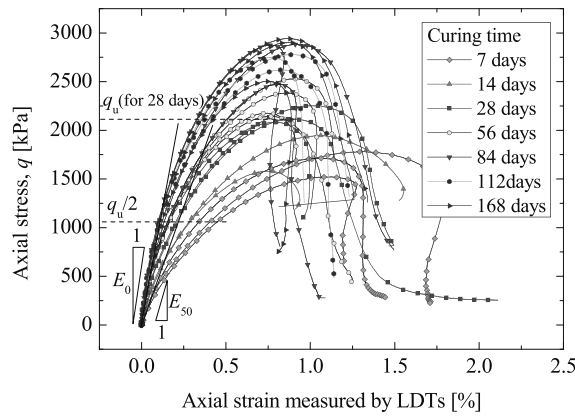


**Figure 6** Stress-strain behaviors of the series UC1

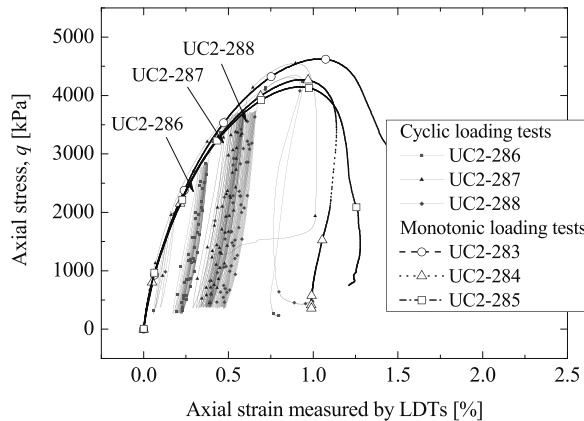


**Figure 7** Stress-strain behaviors in the unconfined cyclic compression tests and the unconfined monotonic compression tests (series UC2)

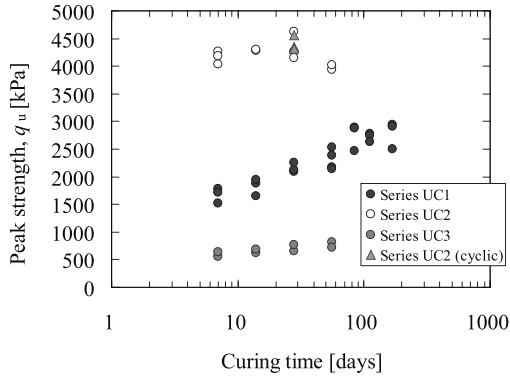


**Figure 8** Variations of peak strength with curing time

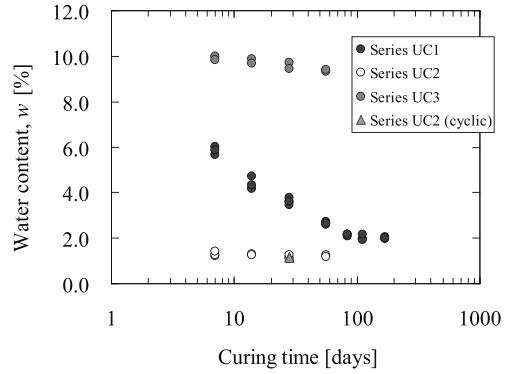


**Figure 9** Variations of water content with curing time

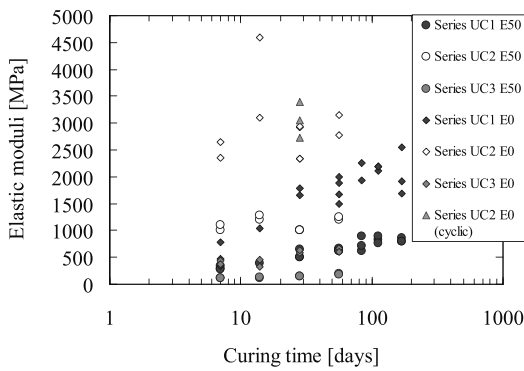


**Figure 10.** Variations of  $E_0$  and  $E_{50}$  with curing time

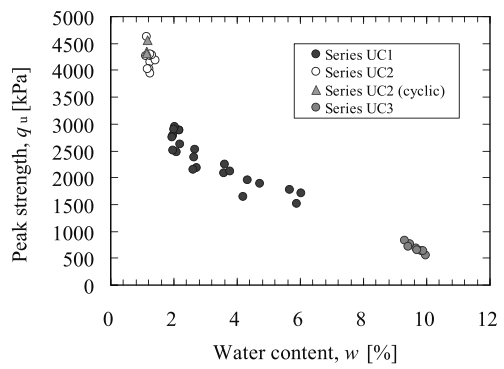


**Figure 11.** Relationship between peak strength and water content

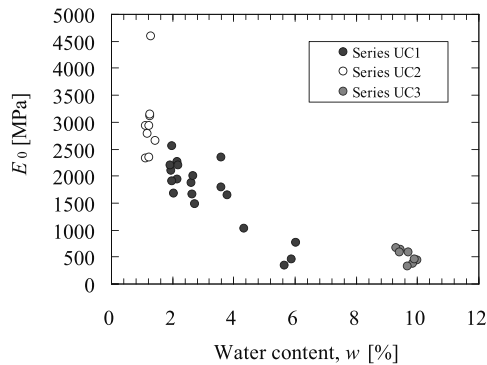


**Figure 12.** Relationship between initial tangent modulus and water content

series UC2 suggest that the demoulded specimens entered into a steady condition after only 7 days curing.

In addition, the peak strength and stiffness did not increase in series UC3 where the water evaporation did prevented during curing. For instance, the peak strength of specimens in the series UC2 having the water content of around 1.24 % was 6.2 times as large as those of specimens in the series UC3 having the water content of around 9.66 %.

**Table 6.** Test results of the series UC2 applied to unconfined cyclic compression test

No.	Loading type	$w$ (%)	Dry density ( $\text{g}/\text{cm}^3$ )	$q_u$ (kPa)	$E_0$ (MPa)
UC2-283	Monotonic	1.13	1.971	4630	2330
UC2-284	Monotonic	1.11	1.950	4270	2930
UC2-285	Monotonic	1.24	1.958	4150	2940
UC2-286	Cyclic	1.14	1.964	4350	3060
UC2-287	Cyclic	1.18	1.958	4560	3390
UC2-288	Cyclic	1.15	1.958	4310	2720

As regards to the cyclic compression tests, the water contents and the dry density of the specimens for cyclic loading tests were almost the same as those of the corresponding specimens for monotonic loading as shown in **Table 6**. The stress-strain behaviors in cyclic loading tests were in good agreement with those in corresponding monotonic loading tests (**Fig. 7**). The values of  $q_u$  of cyclic loading tests were similar to those of monotonic loading tests (**Table 6**). No significant reduction in the peak strength of specimens subjected to large amplitude cyclic loading was observed.

The dependencies of  $q_u$  and  $E_0$  on  $w$  of all the specimens employed for the unconfined compression tests are shown in **Fig. 11** and **Fig. 12**, respectively. A tendency that the  $q_u$  and  $E_0$  values increased as the water content decreases could be seen clearly. As a result, it can be inferred that the strength and the stiffness of the rammed earth material increased as a result of the decrease of water content that induced the increase of suction. In another words, not the curing time but the water content affects predominantly the strength and the stiffness of this type of rammed earth material.

### RESULT OF TRI-AXIAL COMPRESSION TESTS

**Figure 13** shows the stress-strain behavior measured with LDTs. The peak strength increased with confining stress.

The Mohr circles for peak stress conditions are shown in **Fig.14**. The cohesion,  $c$  and the angle of internal friction,  $\phi$ , were evaluated by the  $t - s$  line at peak stress conditions.  $t$  and  $s$  are defined by

$$t = \frac{\sigma_1 - \sigma_3}{2} \quad (1)$$

$$s = \frac{\sigma_1 + \sigma_3}{2} \quad (2)$$

The slope of the line is equal to  $\sin\phi$  and the intercept is equal to  $c \cdot \cos\phi$ . **Figure 15** shows the  $t - s$  line. As the results,  $c$  was evaluated as 626.5 kPa and  $\phi$  was evaluated as 48.9 degrees.

The initial tangent modulus,  $E_0$ , and the secant modulus,  $E_{50}$ , which were measured with LDTs, are shown in **Fig. 16**.  $E_0$  was evaluated with LDTs at a strain level of about 0.001 % and  $E_{50}$  was evaluated with LDTs also (**Fig. 13**). The  $E_0$  and  $E_{50}$  values were rather independent of the confining stress, while the peak strength increased with confining stress as mentioned above (**Fig. 13**). The average value of  $E_0$  and  $E_{50}$  were 1500 kPa and 450 kPa, respectively.



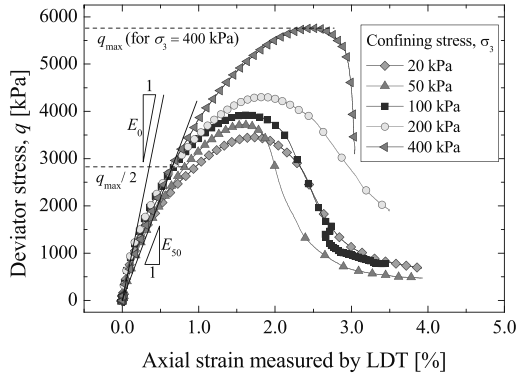


**Figure 13.** Stress-strain behaviors of the series TC

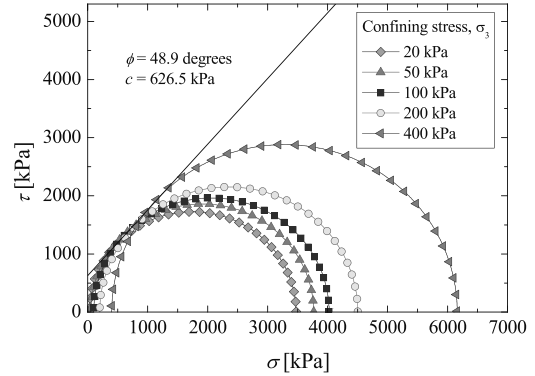


**Figure 14.** Mohr circles for peak stress conditions

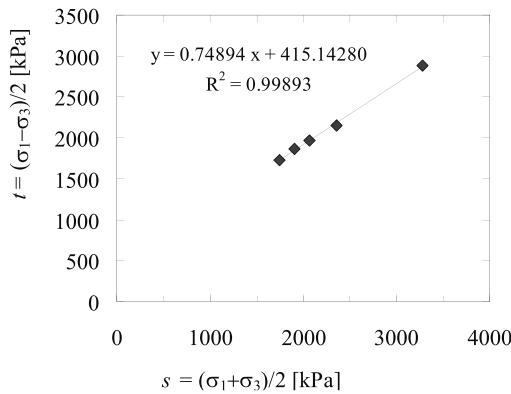


**Figure 15.**  $t$ - $s$  line for peak stress conditions

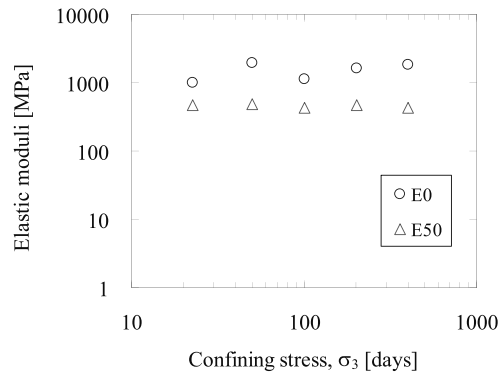


**Figure 16.** Variations of  $E_0$  and  $E_{50}$  with confining stress

## RESULT OF UNCONFINED TENSION TESTS

The stress-strain relationships measured with EDTs and LDTs are shown in **Fig. 17** and **Fig. 18**, respectively. The stress-strain curves based on external and local deformation measurements were totally different from each other. The axial strains measured with EDTs attached at the top cap are overestimated, as they included the effects of bedding errors at the interfaces between the specimen and the top cap and the pedestal and the effects of other system compliances such as the deformation of the lower universal joint. Besides, the apparently horizontal parts that could be seen in the results of tests UT-11 and UT-12 during the initial loading part were also due to the deformation of the universal joint (**Fig.17**).

The failure strains mobilized at the peak stress state range from 0.10 to 0.35% by external measurement which included the above errors. On the other hand, the locally measured strains at failure were smaller than 0.025 %, which were approximately ten times less than the external measurements. Hence the LDTs should be used to evaluate the failure strain, especially in such tension tests.

The stress-strain relationships in cyclic loading tests are shown in **Fig. 19** and **Fig. 20**. The details of the specimens and the test results are shown in **Table 7**. The water contents and dry density of the specimens for cyclic loading tests were almost the same as those of the corresponding specimens for monotonic loading as shown in **Table 7**. The stress-strain behaviors of cyclic loading tests were in good agreement with those of corresponding monotonic loading tests (**Fig. 19** and **20**). The values of

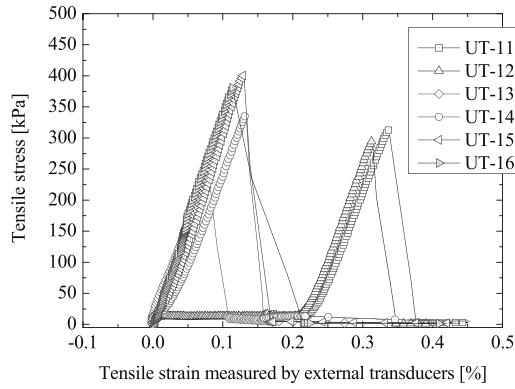


**Figure 17.** Stress-strain behaviors of the series UT measured by EDTs

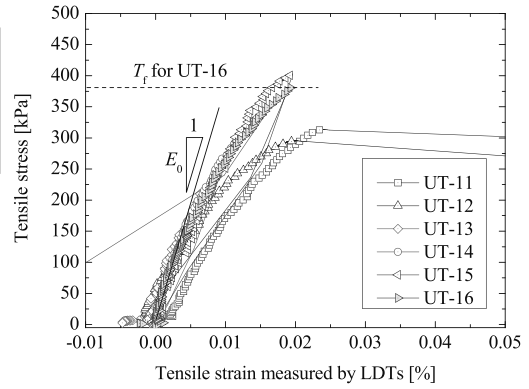


**Figure 18.** Stress-strain behaviors of the series UT measured by LDTs

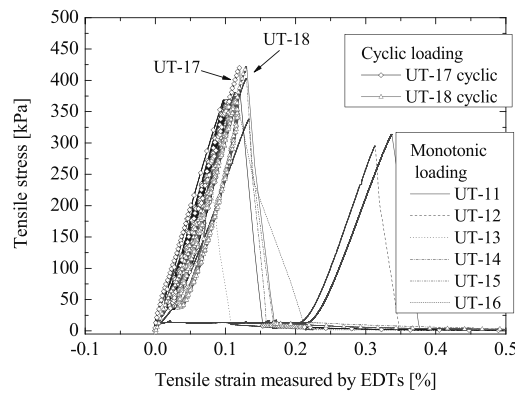


**Figure 19.** Stress-strain behaviors of cyclic loading tests measured by EDTs

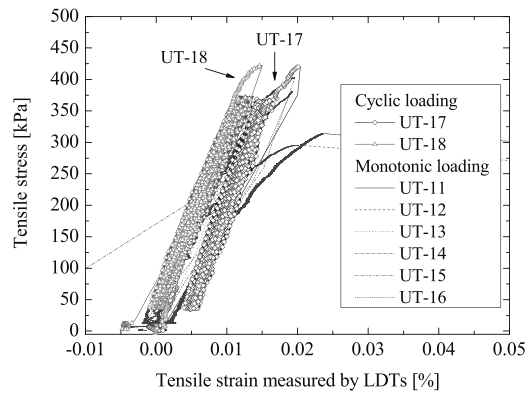


**Figure 20.** Stress-strain behaviors of cyclic loading tests measured by LDTs

**Table 7.** Results of unconfined tension tests

No.	Loading type	$w$ (%)	Dry density ( $\text{g}/\text{cm}^3$ )	$T_f$ (kPa)	$E_0$ (MPa)
UT-11	Monotonic	1.58	1.960	314	1930
UT-12	Monotonic	1.55	1.944	295	2280
UT-13	Monotonic	1.46	1.985	237	2250
UT-14	Monotonic	1.54	1.974	338	2900
UT-15	Monotonic	1.11	1.982	403	1370
UT-16	Monotonic	1.23	1.995	381	3170
UT-17	Cyclic	1.22	1.974	420	2110
UT-18	Cyclic	1.36	1.978	423	3150

$T_f$  evaluated with cyclic loading tests were similar to those evaluated with monotonic loading tests (**Table 7**). No significant reduction in the peak strength of specimens subjected to large amplitude cyclic loading was observed.

For the monotonic loading tests, the average values of the tensile peak strength,  $T_f$  and the initial tangent modulus,  $E_0$  measured by LDTs at a strain level of about 0.001 % were 328 kPa and 2320 MPa, respectively (**Table 7**). The unconfined compression strength of the specimens under almost the same curing condition, i.e., 28 days curing in series UC2, was 4350 kPa (**Table 6**); thus the tensile strength represented less than 10 % of the compressive strength (**Fig. 21**). Whereas the average value of  $E_0$  of unconfined compression test was 2730 MPa; thus  $E_0$  was almost the same in both unconfined

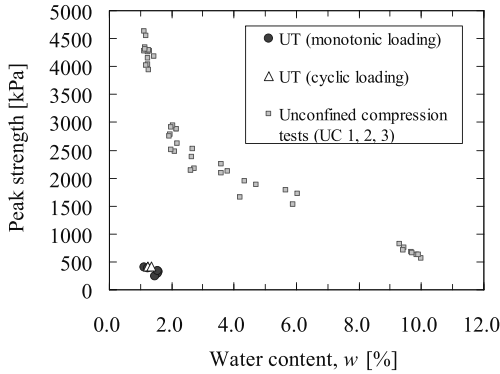


**Figure 21.** Relationship between peak strength and water content

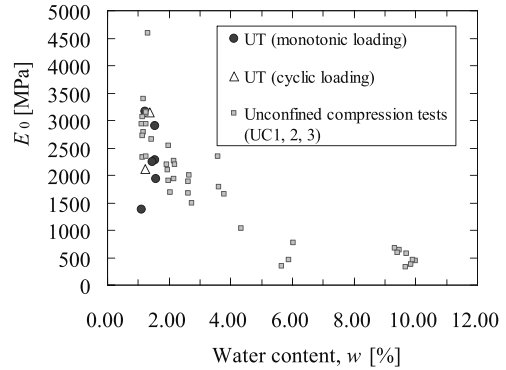


**Figure 22.** Relationship between initial tangent modulus and water content

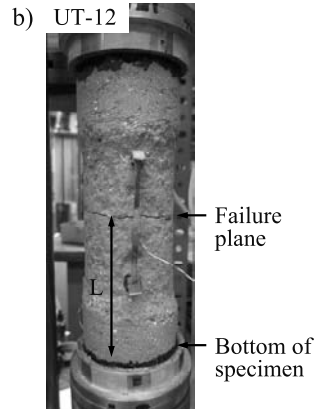
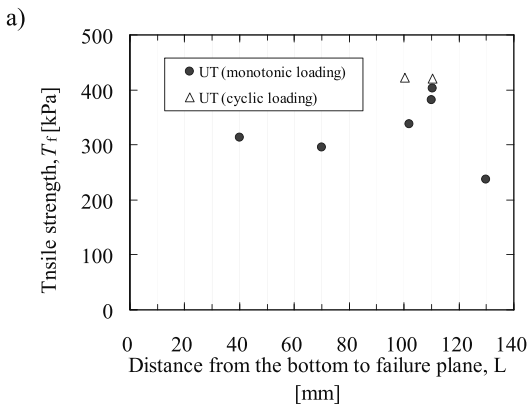


**Figure 23.** a) Relationship between  $T_f$  and distance from the bottom of specimen to failure plane and b) a photo of a specimen after test (UT-12)

compression tests and unconfined tension tests (**Fig. 22**). It is to be noted that the values of water content of specimens for unconfined tension tests and unconfined compression tests were not completely same.

**Figure 23** shows the relationship between  $T_f$  and the distance from the bottom to tensile failure plane,  $L$ . Specimens have layer boundaries at a vertical distance of 10 mm, which were made during the compaction process. All tensile failures occurred at the layer boundaries. Therefore, the  $T_f$  evaluated in the unconfined tension test correspond to the strength of the layer boundary in the specimen.

## CONCLUSIONS

In this paper, unconfined compression tests, unconfined tension tests and tri-axial compression tests were carried out in order to evaluate the tensile and shear strengths of a traditional rammed earth material in Japan. In the unconfined compression tests and unconfined tension tests, some specimens were subjected to large amplitude cyclic loading.

- 1) For the unconfined compression test, the strength and the stiffness increased as a result of the decrease of water content.
- 2) The peak strength increased with confining stress, while the initial tangent modulus,  $E_0$  and the

secant modulus,  $E_{50}$  values were rather independent of the confining stress in the tri-axial compression tests.

- 3) The tensile strength represented about 10 % of the unconfined compressive strength under almost the same curing condition.
- 4) The initial tangent modulus was almost the same in both unconfined compression test and unconfined tension test under almost the same curing condition.
- 5) No significant reduction in the peak strength of specimens subjected to large amplitude cyclic loading was observed in both unconfined compression tests and unconfined tension tests.

## ACKNOWLEDGMENT

The authors would like to thank Nishinomiya city, Hyogo prefecture, Japan, which offered the photo of the rammed earth wall ("Oo-neri bei" in Nishinomiya shrine) collapsed by the 1995 Great Hanshin earthquake disaster.

## REFERENCES

- Goto, S., Tatsuoka, F., Shibuya, S., Kim, Y. S. and Sato, T. (1991). "A simple gauge for local small strain measurements in the laboratory." *Soils and Foundations*, Vol.31, No.1, pp.169-180.
- Hall, M., and Allinson, D. (2009). "Assessing the effects of soil grading on the moisture content-dependent thermal conductivity of stabilized rammed earth materials." *Applied Thermal Engineering*, 29, 740-747.
- Hall, M., and Djerbib, Y. (2004). "Rammed earth sample production: context, recommendations and consistency." *Construction and Building Materials*, 18, 281-286.
- Japanese government's Central Disaster Management Council (2009) "A report on the seismic damage by some scenario inland earthquakes in Kinki and Chubu regions ~a possibility of suffering earthquake on important cultural properties~". No. 21 3-2. (in Japanese)
- Jayasinghe, C., and Kamaladasa, N. (2007). "Compressive strength characteristics of cement stabilized rammed earth walls". *Construction and Building Materials*, 21, 1971-1976.
- Lee, J., Koseki, J., Sato, T., Namikawa, T. and Araki, H. (2010) "Mechanical properties of lime-treated soil and application to earthen walls". *Bulletin of ERS*, No.43, 145-159.
- Minke, G., (2006). *Building with earth: design and technology of a sustainable architecture*, Birkhauser, Germany.
- Namikawa, T. and Koseki, J. (2007) "Evaluation of tensile strength of cement-treated sand based on several types of laboratory tests." *Soils and Foundations*, 47(4), 657-674.
- Onitsuka, K., Chen, P., Tong, P., Negami, T., and Hayakawa, K. (2007). "Geotechnical properties and construction technique of the 'Han-chiku' earth-filled remains located in the Yellow River Valley, China." *Japanese Geotechnical Journal*, JGS, 2(4), 287-295. (in Japanese)
- Rendell, F. and Jauberthie, R. (2009). "Performance of rammed earth structures in east Brittany." *Proceedings of the 11th International conference on Non-conventional Material and Technologies*, Bath, UK.
- Takadachi, A. and Koshihara, M. (2010). "A study of seismic performance of rammed earth wall." *SEISAN KENKYU*, Institute of Industrial Science, Univ. of Tokyo, 62(4), 439-443. (in Japanese)